Article

Ti/Zr/O Mixed Oxides for the Catalytic Transfer Hydrogenation of Furfural to GVL in a Liquid-Phase Continuous-Flow Reactor

Anna Saotta [1,2], Alessandro Allegri [1,2], Francesca Liuzzi [1,2], Giuseppe Fornasari [1,2], Nikolaos Dimitratos [1,2,*] and Stefania Albonetti [1,2,*]

1 Department of Industrial Chemistry "Toso Montanari", University of Bologna, Viale Risorgimento 4, 40136 Bologna, Italy
2 Center for Chemical Catalysis-C3, Alma Mater Studiorum Università di Bologna, Viale Risorgimento 4, 40136 Bologna, Italy
* Correspondence: nikolaos.dimitratos@unibo.it (N.D.); stefania.albonetti@unibo.it (S.A.)

Abstract: This work aims to develop an efficient catalyst for the cascade reaction from furfural to γ-valerolactone in a liquid-phase continuous reactor. This process requires both Lewis and Brønsted acidity; hence, a bifunctional catalyst is necessary to complete the one-pot reaction. Ti/Zr/O mixed oxide-based catalysts were chosen to this end as balancing metal oxide composition allows the acidity characteristics of the overall material to be modulated. Oxides with different compositions were then synthesized using the co-precipitation method. After characterization via porosimetry and NH_3-TPD, the catalyst with equimolar quantities of the two components was demonstrated to be the best one in terms of superficial area (279 m^2/g) and acid site density (0.67 mmol/g). The synthesized materials were then tested using a plug flow reactor at 180 °C, with a 10 min contact time. Ti/Zr/O (1:1) was demonstrated to be the most promising catalyst during the recycling tests as it allowed obtaining the highest selectivities in the desired products (about 45% in furfuryl isopropyl ether and 20% in γ-valerolactone) contemporaneously with 100% furfural conversion.

Keywords: continuous flow; furfural; γ-valerolactone; one-pot reaction; CTH; MPV; Ti/Zr/O mixed oxides

1. Introduction

Furfural (FU), an aldehyde obtained from the dehydration of C5 sugars of hemicellulose, is extremely interesting thanks to its particularly high reactivity, which enables its usage as a platform molecule to obtain numerous high-value-added chemicals [1–3]. The conversion of hexose-based materials such as glucose, cellulose, and alginic acid to furfural was also proved to be viable [4]. However, regardless of the processes and catalysts employed, furfural yields from C6 sugars are much lower than those from C5 ones [5]. Although FU is mostly used to produce furfuryl alcohol (FAL) [6], researchers are trying to develop economically and environmentally convenient processes to produce many other molecules on an industrial scale, such as γ-valerolactone (GVL). GVL is a five-carbon cyclic ester potentially valuable as an additive for bio-based fuels or as a substituent of monomers to produce polymers nowadays derived from oil [7,8]. Nevertheless, due to its extremely high production costs, it is not widely used commercially [7–9]. These are the reasons why developing an economically and environmentally sustainable production of GVL from FU could be of great interest. The process leading from the aldehyde to the ester includes several reaction steps, some catalyzed by Lewis acidity, others by Brønsted acidity (Figure 1) [10–12].
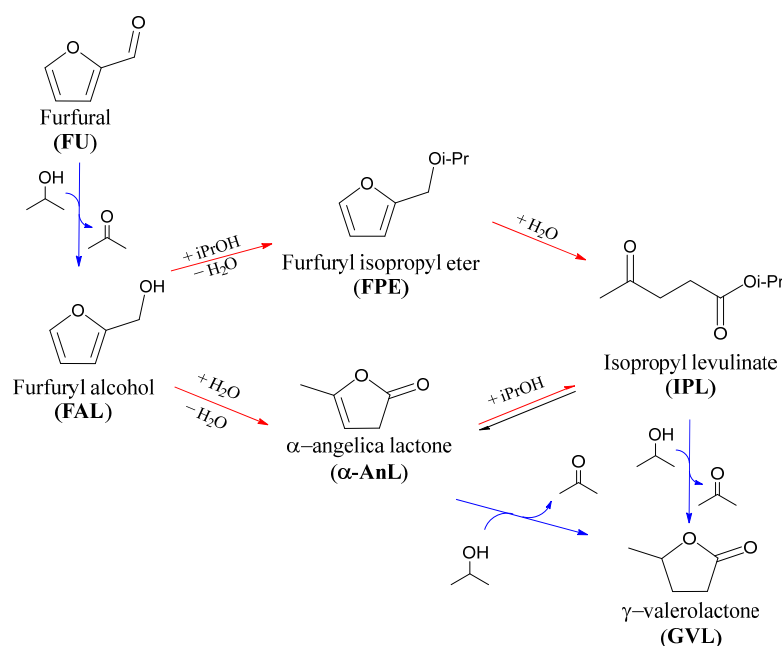
Figure 1. Reaction scheme for the synthesis of γ-valerolactone from furfural. The blue arrows indicate Lewis acidity-catalyzed pathways while the red arrows indicate Brønsted acidity-catalyzed pathways.

Among these steps, there are hydrogenation reactions, which in the biomass-upgrading industry are generally carried out using H_2 due to its wide availability and easy activation on many metal surfaces [13]. Nevertheless, this kind of process requires the use of high pressure [13]. The reason lies in the low solubility of molecular hydrogen in most solvents, which is necessary because of the high boiling points, together with the tendency to decompose upon vaporization, of highly oxygenated molecules [13]. The high pressure inevitably causes safety concerns in addition to the incredibly high infrastructure cost on the industrial scale [13] An alternative approach to H_2 is represented by catalytic transfer hydrogenation (CTH) [6,14]. This mechanism uses an alcohol as a reducing agent, often the same one used as a solvent, and it can be carried out using many types of catalysts, such as metal oxides [15–18], molecular sieves [19,20] and metal–organic frameworks [21–23], instead of noble metal catalysts necessary in the classical hydrogenation. However, to facilitate the CTH between an alcohol and a carbonyl group, acid–base pair sites are needed [13]. Lewis acid-type and Lewis base-type catalysts, such as Zr-based or Mg-based ones, are often used for this reason [24] as a synergistic effect of the two types of sites to simultaneously activate both the carbonyl group and the alcohol is needed [25]. The Lewis acid site, typically an electron-deficient metal center, is necessary to bond with the electron-rich oxygen in the carbonyl group of the acceptor. Additionally, it interacts with the hydroxyl oxygen of the hydrogen donor. The adjacent basic site, instead, attracts the proton in the hydroxyl, weakening the O–H bond. Consequently, strong basic sites can effectively abstract the hydrogen from the hydroxyl group of the alcohol, promoting the hydride transfer. Equally, the hydrogen removal by the base site will be easier with stronger Lewis acid sites that make the hydroxyl hydrogen in the hydrogen donor more acidic. Hence, both acid and base sites are required for the CTH [13]. CTH not only allows the use of both high H_2 pressure and precious metal catalysts to be avoided [15], but also enhances the solubility of the hydrogen donor in liquid-phase reactions, making the experimental setup both less complex and less expensive [13]. One more advantage of using CTH can be seen in the lower hydrogenating capability of most organic hydrogen donors in comparison with H_2, which enables an easier control of selective hydrogenation when partially hydrogenated molecules are desired [13]. Although substantial hydrogenation facility modification would be surely needed [13], the advantages in using CTH rather than H_2 to reduce biomass-derived molecules are not negligible. Moreover, the choice of an appropriate reducing agent, together with the use

of a suitable heterogeneous catalytic system, is of great interest for the one-pot reaction in analysis as it can eventually lead to the implementation of a more sustainable process. In fact, many studies can be found regarding the application of CTH to the cascade reaction. The latter is typically performed in batch processes using a secondary alcohol (mainly isopropanol) as a H-donor and Zr/Al-based catalysts (usually zeolites) [16,26–29]. Melero and co-workers systematically studied the feasibility of this process in batch over bifunctional catalysts, demonstrating its realization and optimizing the reaction conditions not only starting from FU [29] but also starting from xylose [9,27,29]. After identifying the catalyst system with the best performance (Al/Zr ratio of 0.22), which successfully produced 35 mol% of GVL from xylose (30.5 g L^{-1}), they also performed a rational optimization of the catalyst synthesis and reaction conditions, concluding that tuning the Brønsted/Lewis acid site ratio is a key aspect for the good efficiency of the process [9,27]. Despite the great results obtained working in batch mode, a very low number of reports are present in the open literature regarding the cascade reaction in continuous flow, even though it has been demonstrated that the batch-to-continuous transition for the production of large-volume specialty chemicals yields strong process intensification benefits [30]. Indeed, performing under flow conditions can provide shorter reaction time, fast reagent mixing, better heat transfer, simpler downstream processing, easier scale-up and increased reactor volume productivity [31]. C. López-Aguado et al., studied the cascade reaction in continuous mode using furfural as a substrate and Zr-modified dealuminated beta zeolite as a catalyst [30]. Although a 40 mol% yield of GVL was initially obtained working with a contact time of 5 min g mL^{-1}, the catalyst was quite unstable. Hence, due to the fouling of Al, it deactivated within 6 h of reaction [30]. Better results were obtained using levulinic acid (LA) as a raw material (GVL yields > 90% at 170 °C, 100% of LA conversion, demonstrated long-term stability of the Zr-Al-Beta catalyst) [30]. Nonetheless, the efficient production of GVL from an aldehyde in continuous flow remains challenging. Herein, we have investigated the conversion of FU to GVL using isopropanol as a H-donor and solvent in a liquid-phase continuous reactor. Ti/Zr/O mixed oxides with different composition were chosen as catalytic systems to this end. As a matter of fact, zirconia is reported to be highly efficient in hydrogenating FU due to its strong Lewis acidity [12,18,32,33], which also favors the last step of the one-pot reaction. However, being characterized by weak Brønsted acidity [4,18], this oxide is unable to catalyze the entire cascade reaction. Since it has been demonstrated that mixing two dissimilar oxides allows obtaining different physiochemical properties and catalytic behavior depending on the quantities of the two components [18], anatase-type TiO_2 was chosen to be mixed with ZrO_2 because of the effective isovalent substitution, similar electronegativity and ionic radius [34]. TiO_2 is well known for its photocatalytic and strong metal support interaction (SMSI) properties [18,35]. By mixing titania with zirconia, the best characteristics of the two oxides can be obtained in a single material [18]. This combination has already been widely used in many fields [36], such as in the catalytic dehydrogenation of ethylbenzene or in the production of ε-caprolactam [18]. Some works regarding biomass valorization are also present [36]; for instance, the efficient hydrogenation of alkyl levulinates to γ-valerolactone [6,35] or the self-condensation of cyclopentanone [37] can be mentioned.

2. Materials and Methods

2.1. Subsection

$ZrO(NO_3)_2 \bullet 2H_2O$ (Sigma Aldrich, St. Louis, MO, USA, 25%) and $TiOSO_4 \bullet xH_2O$ (Sigma Aldrich, 25%) were used as precursors in the Ti/Zr/O mixed oxide synthesis. The substrates used to examine the one-pot reaction were furfural (Sigma Aldrich, 98%), furfuryl alcohol (Sigma Aldrich, 98%), furfuryl ethyl ether (Sigma Aldrich, 98%), α-angelica lactone (Sigma Aldrich, 98%), propyl levulinate (Sigma Aldrich, 95%) and γ-valerolactone (Sigma Aldrich, 99%). Isopropanol (Sigma Aldrich, 99.5%) was used as solvent and octane (Sigma Aldrich, 99%) as standard for GC-FID analysis. SiC (silicon carbide) powder was used as diluent for the continuous-flow reactor.

2.2. Synthesis of Catalysts

A precipitation method at controlled pH ($\approx$9–10) was used as reported in the literature [25], and it was appropriately modified for this work to obtain high-surface-area zirconia. An aqueous solution of zirconium (0.3 M) was prepared; its volume was calculated to yield 12 g of zirconia at the end of the process. An aqueous solution of ammonia (5 M) was also prepared considering that the desired molar ratio of NH_3/Zr was equal to 10. After the desired volume of the aqueous solution of ammonia was transferred to a round-bottom flask, the desired amount of the aqueous solution of zirconium was added dropwise under vigorous stirring. Once the addition was complete, the round-bottom flask was equipped with a thermometer, a water condenser and a Teflon feeding line reaching under the liquid surface. The mixture was then heated to its boiling point with a silicone bath set at 110 °C and was kept boiling under vigorous stirring for 48 h. To keep the pH in the 9–10 range for the whole 48 h, the feeding line was connected to a syringe pump feeding 2.7 mL/h of concentrated ammonia (26 M) to the system. After the digestion was completed, the mixture was allowed to cool to room temperature, and the slurry solution was filtered using a Buchner funnel and thoroughly washed with 1 L of 3 M ammonia aqueous solution. The resulting solid was dried at 100 °C overnight and then ground and calcined at 500 °C for 12 h, with a heating rate of 5 °C/min for one hour and fifteen minutes. After calcination, the materials were cooled with a ramp of 10 °C/min down to room temperature.

To synthesize Ti/Zr/O mixed oxides, the same procedure described for zirconia was used, except for the substitution of an appropriate amount of zirconium precursor (zirconium oxynitrate) with titanium oxysulfate, always keeping the total concentration of metals [Zr] + [Ti] = 0.3 M in a single solution, and the molar ratio $NH_3/(Zr + Ti)$ = 10. The [Ti]/[Zr] molar ratios employed, reported next to the names of catalysts between brackets as in Table 1, were 1/3, 1/1, 2/1 and 3/1. A reference sample of titania was synthesized using the same procedure for catalytic comparison.

Table 1. Atomic content, surface and acid properties based on strength and acid site density for the Ti/Zr/O synthesized catalysts, using XRF, BET and TPD-NH_3, respectively.

Sample	Ti Atomic Content (%)	Zr Atomic Content (%)	BET $_{SSA}$ (m^2/g)	Acid Site Density (mmol/g)	T_{max} NH_3 Desorption (°C)
ZrO_2	0	100	250	0.49	291
Ti/Zr/O (1:3)	27.8	72.2	268	0.51	278
Ti/Zr/O (1:1)	46.5	53.5	279	0.67	237
Ti/Zr/O (2:1)	67	33	287	0.54	267
Ti/Zr/O (3:1)	74.5	25.5	330	0.62	263
TiO_2	100	0	60	0.25	367

2.3. Characterization of Catalysts

The composition of the Ti/Zr/O oxides was analyzed through X-ray fluorescence (XRF) with a PANalytical Axios Advantage instrument. Catalyst crystalline phases were identified by X-ray powder diffraction (XRD), using a Bragg/Brentano diffractometer (X'pertPro PANalytical) equipped with an X'Celerator detector and Cu-Kα (λ = 1.5418 Å) radiation. The diffractograms were recorded in the 5° < 2θ < 80° range, with a 0.05°2θ acquisition step and 600 s acquisition time. Textural parameters (S_{BET}, V_P and D_P) were assessed via N_2 adsorption–desorption porosimetry using a Sorpty 1750 Fison instrument. Prior to cooling in a liquid nitrogen bath for N_2 adsorption, samples were outgassed at 200 °C. Surface areas were determined by using the Brunauer–Emmett–Teller (BET) equation assuming a cross section of 0.162 nm for the nitrogen molecule. The pore size distribution was obtained using the Barrett–Joyner–Halenda (BJH) model. Temperature-programmed desorption of ammonia (NH_3-TPD) was used to determine the density of acid sites. Firstly, 0.2 g of each catalyst was evacuated in a He flow from room temperature

to 500 °C, with a rate of 10 °C/min, and cooled under the same conditions to 100 °C during the so-called "degas" phase. The adsorption of NH_3 followed, using 10% of NH_3 in He flow for 20 min. Then, He flow was passed to carry out the physiosorbed ammonia. Finally, temperature-programmed desorption was performed by heating the samples from 100 to 500 °C at a heating rate of 10 °C/min. A thermal conductivity detector (TCD) was used to quantify the desorbed ammonia.

2.4. Catalytic Tests

Continuous-flow reactions were carried out using a homemade liquid-phase fixed-bed reactor (Figure 2). SiC as the desired diluent was loaded into the reactor together with 1 mL (between 0.76 and 0.94 g) of catalyst placed within the isothermal zone of the oven.
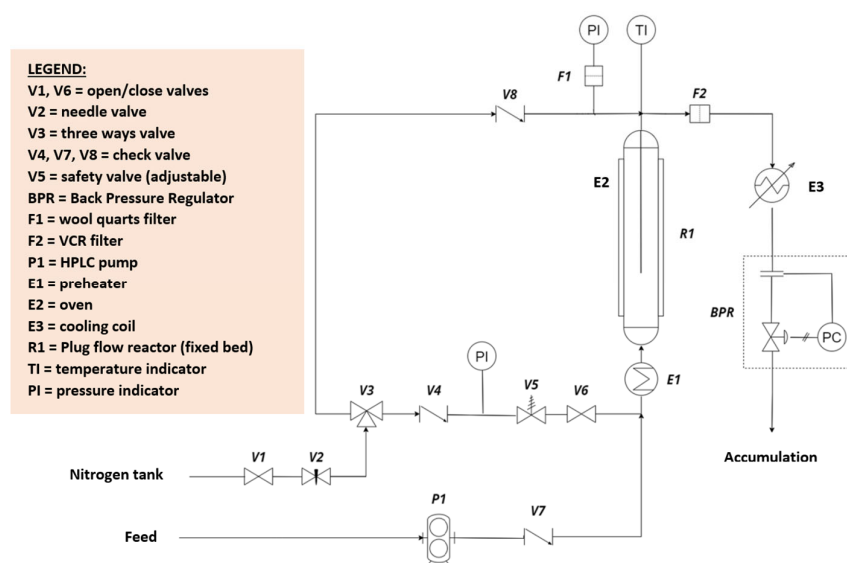

Figure 2. Scheme of the liquid-phase continuous plant used.

The diluent and the catalysts were sieved before (d > 60 and 80 < d < 60 mesh, respectively) to facilitate their separation at the end of the reaction. The reactor was then pressurized to 40 bar with N_2. This pressure was chosen to prevent boiling of the solvent at the desired reaction temperature, and the reaction mixture was fed into the reactor with a flow rate of 0.3 mL/min with an HPLC pump (JASCO PU4080i) until the flow out of the BPR was stable and without the presence of gas bubbles. After making sure to avoid and eliminate any back-mixing phenomena, the feed flow was reduced to 0.1 mL/min and both the preheater and oven were turned on. To minimize temperature gradients within the reactor, the oven was set at the reaction temperature, while the preheater was set at a 15% higher temperature. In particular, for reactions carried out at 180 °C, the oven was set at 180 °C, and the preheater at 207 °C. A 67 mM furfural solution in isopropanol, containing an equivalent of H_2O and 330 µL of octane, used as internal standard, was prepared in a 250 mL flask to be used as feed. The samples were collected every hour at the end of the system in a 10 mL volumetric flask, diluted to volume with isopropanol and analyzed via gas chromatography (Clarus 500 della Perkin Elmer) using a flame-ionization detector (GC-FID). The analysis method used was as follows: injector heated to 250 °C for the vaporization of the mixture, with a He flow as eluent of 1.2 mL/min and split ratio equal to 30; Agilent HP-5 column (diameter 0.32 mm, length 30 m) placed inside a heated chamber at a controlled temperature through the following temperature program: 2 min of isotherm at 50 °C, heating of 10 °C/min up to 250 °C and isotherm of two minutes at 250 °C; FID detector heated to 250 °C for compound detection. To calculate the response factors, the moles, hence the molar flow, and finally the conversion and selectivities of the different products obtained, calibration curves of the principal commercial molecules involved in the

cascade reaction (FU, FAL, α-AnL, β-AnL, FPE, GVL and IPL) were evaluated. In this way, retention times were identified: 5.0, 5.3, 5.7, 6.7, 6.8, 7.0 and 9.3 min, respectively. Furfural conversion, product selectivities and the percentage of undesired products (others) were calculated according to Equations (1)–(3), respectively:

$$Conversion(\%) = \frac{[\tilde{V}_{FUi}\left(\frac{mol}{min}\right) - \tilde{V}_{FUf}\left(\frac{mol}{min}\right)]}{\tilde{V}_{FUi}\left(\frac{mol}{min}\right)} \times 100 \tag{1}$$

$$Selectivity_X(\%) = \frac{\tilde{V}_X\left(\frac{mol}{min}\right)}{[\tilde{V}_{FUi}\left(\frac{mol}{min}\right) - \tilde{V}_{FUf}\left(\frac{mol}{min}\right)]} \times 100 \tag{2}$$

$$Others(\%) = 100 - \sum Selectivities \tag{3}$$

$\tilde{V}_{FUi}$ and $\tilde{V}_{FUf}$ are the initial and final molar flows of furfural (mol/min), while $\tilde{V}_X$ is X (where X identifies a certain product) molar flow (mol/min). All results are expressed as percentages.

3. Results and Discussion

3.1. Physicochemical Properties of the Catalysts

Ti/Zr/O materials were synthesized by employing the procedure described in Section 2.2 and varying the relative molar ratio of the two cations. To verify that the Ti/Zr molar ratios were the ones desired, X-ray fluorescence was used. The results obtained, reported in Table 1, showed that the values of the nominal Ti/Zr composition are in good agreement with the actual values of the measured Ti/Zr composition, confirming the reliability of the experimental procedure for the synthesis of Ti/Zr/O materials in a wide range of different compositions. The XRD profiles of ZrO_2 and Ti/Zr/O having different compositions (calcined at 500 °C as the optimum temperature to obtain the desired crystalline phase, Figure S1) are shown in Figure 3. Zirconia, together with all mixed oxides, was found to be amorphous at this calcination temperature. In fact, no sharp diffraction peaks are evident, but two broad diffraction peaks respectively in the (20–40)°2θ and (40–70)°2θ ranges can be distinguished (Figure 3a). Given that no ZrO_2 or TiO_2 diffraction peaks are present, a homogeneous distribution of the oxides can be implied [38]. The results are in line with literature findings [18,37–40]. Titania is the only one to have a crystalline structure after having been calcined at 500 °C, as is evident from the sharp, clear diffraction peaks in Figure 3b. In particular, the diffraction peaks observed at 25.3°, 37.0°, 37.8°, 38.6°, 48.1°, 53.9°, 55.0°, 62.7°, 68.7°, 70.3°, 74.0°, 75.0° and 76.0° (Figure 3b) correspond to the (101), (103), (004), (112), (200), (105), (211), (204), (116), (220), (107), (215) and (301) tetragonal crystal planes of the anatase phase of TiO_2, in agreement with previous literature [41–44].
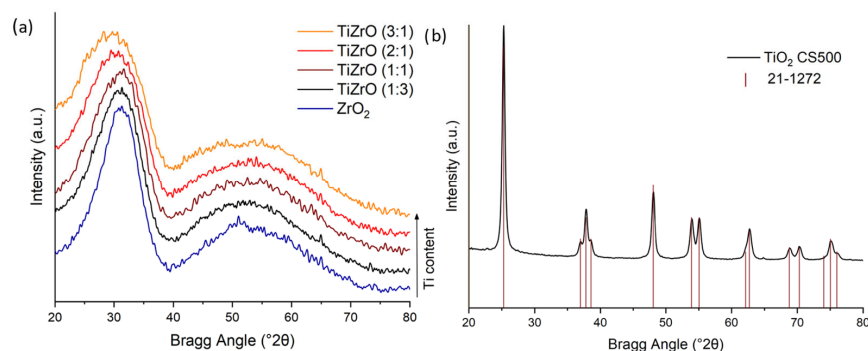

Figure 3. (**a**) Diffractograms obtained from XRD analysis of the mixed oxides Ti/Zr/O (3:1), Ti/Zr/O (2:1), Ti/Zr/O (1:1), Ti/Zr/O (1:3) and ZrO_2; (**b**) diffractograms obtained from XRD analysis of the mixed oxide TiO_2.

The specific surface area of each sample was calculated using the BET equation (Table 1). The values obtained were in the 250–330 m^2/g range, highlighting no significant difference between the different samples, but demonstrating a high flexibility of the synthetic procedure in maintaining a high surface area across a vast range of compositions. Titania is the only exception as it displayed a low surface area compared to the other materials of the series, equal to 60 m^2/g, in agreement with the literature [39]. Furthermore, it can be noticed that the BET superficial area of the mixed oxide increases with the Ti content. Lin et al. [39] reported the same trend we noticed. However, both Lu et al. [43] and Masahiro et al. [45] had different results, observing the maximum superficial area in titania–zirconia mixed oxide with equimolar quantities. The different results may be due to the different phases analyzed given that the present study, as well as that of Lin et al. [39], worked with the amorphous phase of Ti/Zr/O, while Lu et al. [43] and Masahiro et al. [45] studied crystalline phases of the same mixed oxides. In Figure 4a, profiles obtained from NH_3-TPD analysis are shown.
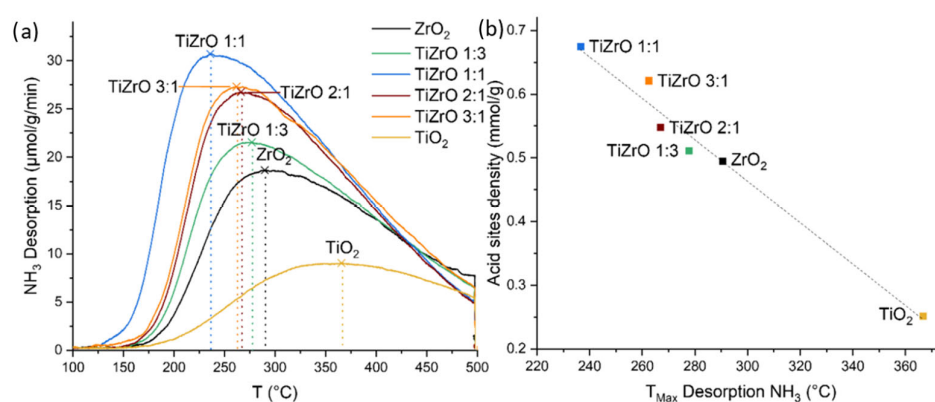

Figure 4. (**a**) TPD-NH_3 profiles and (**b**) acid site density as a function of the maximum temperature of NH_3 desorption for the synthesized mixed oxides.

NH_3-TPD analysis was used to measure the strength and density of total acid sites (Table 1). The acid site density is represented by the underlying area of the desorption profiles shown in Figure 4a, and titania showed the lowest value, equal to 0.25 mmol/g. Zirconia, despite being characterized by almost double the acid site density of titania (0.49 mmol/g), was still less acidic than the mixed oxide materials, which showed values of a relatively high density of acid sites, in the 0.51–0.68 mmol/g range. The significant increase in surface acidity of mixed oxides with respect to the single components, particularly in the case of Ti/Zr/O, has already been highlighted in the literature [18,46]. Previous studies identify the cause of the development of a great number of acid sites in the mixed oxides as the substitution of some titanium by zirconium atoms, or the effect of large dispersion of TiO_2 or ZrO_2 on the surface of the mixed oxide [46]. In agreement with previous studies, in the present work, Ti/Zr/O (1:1) reached the maximum value [18,45,46] (0.68 mmol/g). From the desorption profiles, the maximum temperature of NH_3 desorption, indicative of the strength of the acid sites [46], could also be obtained. Figure 4b shows the acid site density as a function of the maximum temperature of NH_3 desorption (results are also reported in Table 1), showing an interesting trend. The highest density of acid sites seems to be associated with the lowest maximum temperature of NH_3 desorption. Consequently, titania, despite being the material with the lowest acid site density, showed the highest maximum temperature of NH_3 desorption at 367 °C, much higher than the values found for the other materials. It appears that by doubling the density of acid sites (from TiO_2 to ZrO_2), the maximum of the desorption peak was shifted substantially from 367 °C to 290 °C. This trend is observed for the series of catalysts, up to Ti/Zr/O (1:1), which had the maximum desorption peak at 237 °C, the lowest value in the series of presented catalysts. Manríquez et al., observed a similar trend [46].

3.2. Catalytic Results

Ti/Zr/O-based catalysts were tested in a continuous liquid-phase fixed-bed reactor to evaluate their catalytic performance in the one-pot reaction, as shown in Figure 5. The blank test only with the use of diluent resulted in negligible conversion, as shown in Figure S4. The first step of the cascade reaction consists in the reduction of FU to FAL through CTH of isopropanol (iPrOH). The specific mechanism through which the alcohol is formed is called the Meerwein–Ponndorf–Verley (MPV) mechanism [35]. To facilitate the process, the alcohol used is commonly the same alcohol that acts as a solvent. Subsequently, Brønsted acidity is required to allow the formation of FPE through etherification [47], which is likely to be the predominant species given the high concentration of alcohol (iPrOH). The next step involves the hydrolytic opening of the ring of both FAL and FPE to levulinic acid (LA) and isopropyl levulinate (IPL), respectively. These two molecules are in equilibrium with each other and can both be reduced through another H-transfer reaction (MPV mechanism) to form 4-hydroxypentanoic acid and isopropyl 4-hydroxypentanoate. The high instability of the last two compounds leads to their immediate conversion to GVL. Given the high concentration of the iPrOH, the path comprising FPE, IPL and HIP is most likely to be predominant. In addition, another parallel reaction is possible, both from FU and FAL [28,48]. The reaction produces α- and β-angelica lactones (AnL), in equilibrium with each other, which require the reduction of the double bond to be converted into GVL afterward. In this work, the final aim is to obtain GVL from FU.

The FU conversion to GVL was previously studied in the temperature range of 150–190 °C [9,29,47,49]. In this work, all tests were carried out at 180 °C and 0.1 mL/min flow rate, so as to have a contact time of 10 min. The choice to use a contact time higher than general values reported in the literature is due to the different substrate used, as many started from levulinate esters [30]. However, after a first screening phase, the effects of the temperature and contact time on the catalytic performance were also evaluated. However, first of all, the effect of the "time on stream" (i.e., the time in which the catalyst is in contact with the reagent flow) on the catalytic activity of the different oxides was studied, and the tests were performed over a long period of time (about 52 h). Figure 7 shows, as an example, the test performed on the Ti/Zr/O (1:1) sample. In particular, the graph shows the trend of furfural conversion (X FU) and selectivity in the main products (furfuryl alcohol "FAL", furfuryl isopropyl ether "FPE", angelic lactone "AnL", isopropyl levulinate "IPL" and γ-valerolactone "GVL") as a function of the reaction time in hours (h). Other undesired compounds, which justify the loss of carbon atoms compared to the initial ones at the end of the reaction, were formed. Some of them were identified (Figure 6) through GC and mass spectroscopy (MS) analysis. The main products were isopropyl furan-2-carboxylate, 4-(furan-2-yl)but-3-en2-one (or furfuryldenacetone) and di(furan-2-yl)methane, but these products could not be calibrated and quantified because they are not available commercially. The origin of the first compound has not yet been defined with certainty. In contrast, the second by-product derives from the aldol condensation of FU with acetone, in turn produced by the CTH [50]. The third one, instead, derives from secondary reactions on FU towards its oligomerization [7].

Figure 7 shows the catalytic performance of the Ti/Zr/O (1:1). The catalytic performance was found to be stable. Characterization of the fresh and used catalyst based on XRD and surface area analysis confirms this stability as it showed the characteristic diffraction peaks with a slight change in the intensity and a small decrease in surface area, therefore showing good structural stability (Figure S2). For the whole series of samples, surface area analysis showed a small to medium decrease in specific surface area, mean pore volume and mean pore diameter after their utilization, probably indicating the adsorption of intermediates and products and fouling (Table 2). These data, acquired through porosimetry, show that the differences between the fresh and used catalysts are in the 17–84 m^2/g range for superficial area, 0.06–0.42 cm^3/g range for mean pore volume and 0.3–2.8 nm range for mean pore diameter. Figure 8 shows the comparison of the mean catalytic results obtained (every test lasted 52 h).
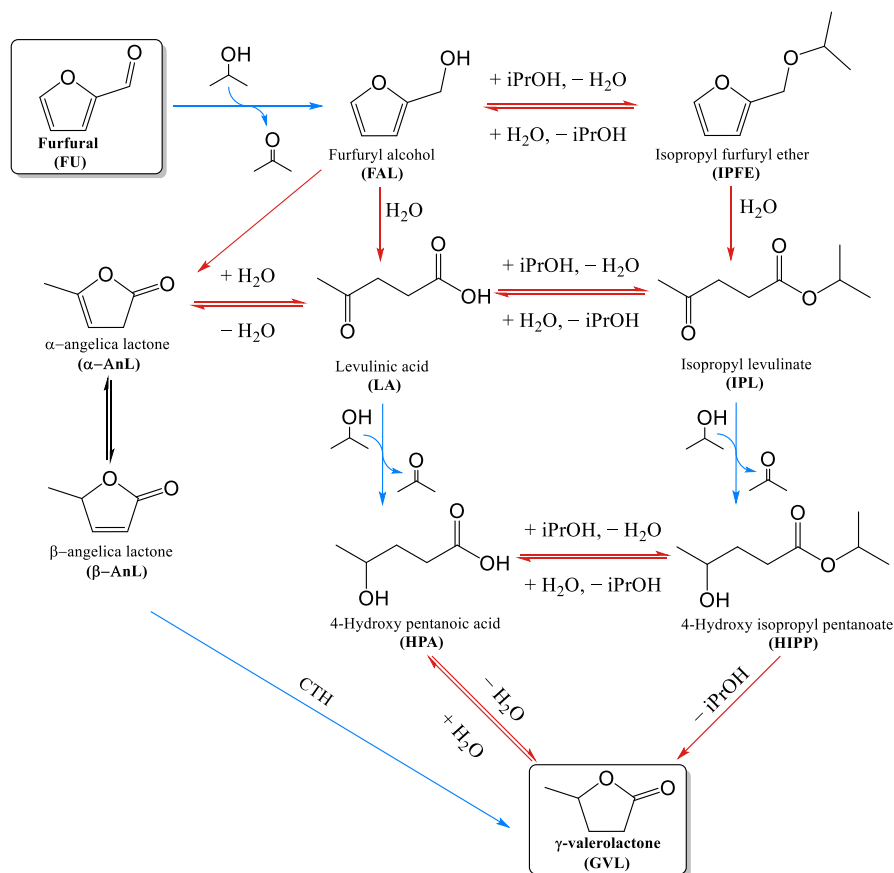
Figure 5. Detailed reaction scheme for the synthesis of γ-valerolactone from furfural. The blue arrows indicate Lewis acidity-catalyzed pathways while the red arrows indicate Brønsted acidity-catalyzed pathways.
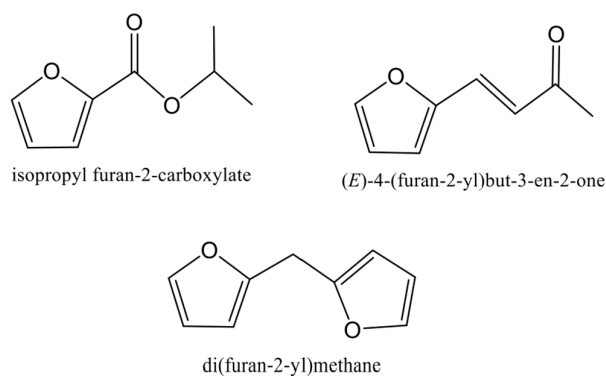

Figure 6. Undesired products formed from one-pot reaction from FU to GVL.
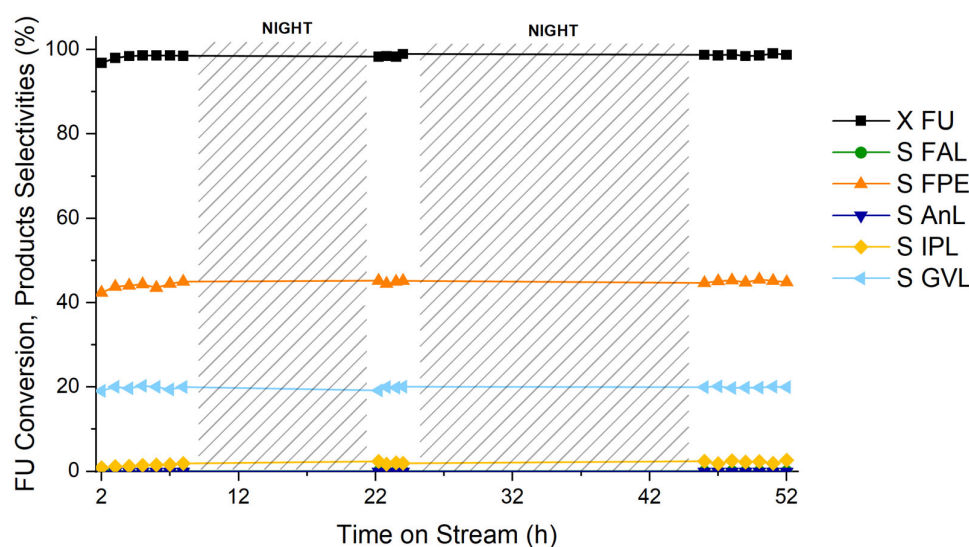
Figure 7. Furfural conversion and product selectivities (%) with respect to the time on stream (h) using Ti/Zr/O (1:1). Reaction conditions: [FU] = 67 mM, τ = 10 min, T = 180 °C, m_{cat} = 0.76 g.

Table 2. Specific surface area, mean pore volume and mean pore diameter of the Ti/Zr/O mixed oxide with different compositions obtained through BET and BJH equations; comparison between fresh and used (spent) catalysts.

Sample	BET $_{SSA}$ (m^2/g)		Vpores (m^3/g)		Dpores (nm)	
	Fresh	Spent	Fresh	Spent	Fresh	Spent
ZrO$_2$	279	248	0.37	0.31	4.6	4.3
Ti/Zr/O (1:3)	268	184	0.62	0.31	8.5	6.1
Ti/Zr/O (1:1)	279	220	0.66	0.34	8.4	5.6
Ti/Zr/O (2:1)	287	213	0.81	0.39	9.9	6.4
Ti/Zr/O (3:1)	330	190	0.56	0.28	5.8	5.0
TiO$_2$	78	61	0.16	0.11	7.0	5.3

Considering the overall trend of the different catalysts (Figure 8), it is evident that the selectivity in FAL decreases with the increase in the amount of Ti from ZrO$_2$ to Ti/Zr/O (3:1) and increases again when TiO$_2$ is used (Figure S6); selectivities in FPE and GVL have a bell-shaped trend, increasing from ZrO$_2$ up to the mixed oxide Ti/Zr/O (1:1) and then gradually decreasing to the opposite extreme; selectivities in AnL and IPL are minimal (<3%), while furfural conversion is high in all cases (>94%) Although the main products obtained are FAL, FPE and GVL, some other unexpected compounds are formed. GC-MS was useful to identify some of them, as reported before in this section, such as isopropyl furan-2-carboxylate, 4-(furan-2-yl)but-3-en2-one (or furfuryldenacetone) and di(furan-2-yl)methane (Figure 6). This is the reason why the sum of the selectivities is not 100%. Working with ZrO$_2$, a high selectivity in FAL is evident (55%) (Figure S5). This result is in line with the expectations, given that the hydrogen transfer requires high Lewis acidity, which is characteristic of this oxide, as is reported in the literature [12,18,32,33]. Contrarily, the selectivities in subsequent reaction products, namely FPE, AnL, IPL and GVL (Figure 5), which require Brønsted acid catalysis to be formed, is less than 10% in every case. As zirconia is primarily a Lewis acid, it lacks suitable sites to effectively catalyze the successive steps of the reaction [10,33]. The mixed oxide Ti/Zr/O (1:3) shows similar results to zirconia, and the highest selectivity is still in FAL (30%). The reason probably lies in the major quantity of Zr present in this material. However, the presence of Ti in the mixed oxide became important as an increase in selectivity in post-FAL products is observed (FPE 18%, GVL 7%). The catalyst with equimolar composition, Ti/Zr/O (1:1), exhibits the highest values of selectivity in FPE and GVL, 45% and 20%, respectively, and

has minimal selectivity in FAL, AnL and IPL (all <2%). The two mixed oxides richer in Ti atomic content show a very similar reaction pattern, with a decrease in the selectivity of the desired products ($S_{FPE} \approx 40\%$ and $S_{GVL} \approx 16\%$) compared to Ti/Zr/O (1:1). Finally, using TiO$_2$, the selectivity of the desired products continues to decrease ($S_{FPE} \approx 31\%$ and $S_{GVL} \approx 8\%$). A slight increase in FAL selectivity (4%) is also evident. Given the results, Ti/Zr/O (1:1) was found to be the best catalyst for the one-pot reaction among the ones investigated in the reaction conditions chosen. Its catalytic performance could be attributed to its high values of density of acid sites (mmol/g) and specific surface area. The results imply that this is the catalyst characterized by the most suitable B/L acidity ratio among the ones investigated, even if we cannot confirm this due to the inability to measure it. However, despite mainly Lewis acids being present [37,51], the presence of Brønsted acid sites on Ti/Zr/O mixed oxide has been previously reported [37,45].
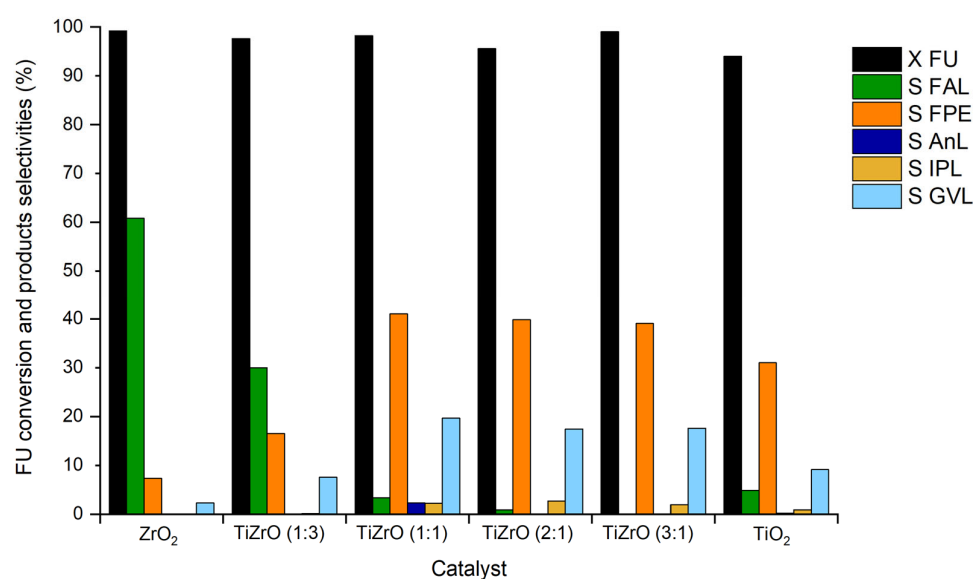

Figure 8. Catalyst performance comparison for the one-pot reaction from furfural to γ-valerolactone. Reaction conditions: [FU] = 67 mM, τ = 10 min, T = 180 °C, m$_{cat}$ between 0.76 and 0.94 g.

3.3. Influence of the Reaction Conditions

Since the mixed oxide Ti/Zr/O (1:1) shows the best catalytic performance (Figure 7), this catalyst was chosen to study the influence of reaction conditions on catalytic performances and analyze the reaction mechanism. In particular, the effects of temperature and contact time were evaluated. Firstly, the effect of reaction temperature on average catalytic performance, calculated over 52 h of reaction, was considered (Figure 9) by testing the Ti/Zr/O (1:1) at 180 °C and 150 °C (τ = 10 min). A lower reaction temperature with respect to the previous tests was tried to verify if complete FU conversion with slightly lower selectivities were obtainable at less severe experimental conditions. The results (Figure 9) highlight how the conversion of FU does not change with the temperature, remaining complete even in milder conditions, while there is a significant difference in the selectivity of the products. The explanation for this behavior lies in the very nature of the oxides under analysis. These, in fact, are basically Lewis acids [37,51]; hence, the conversion of aldehyde to alcohol is in any case very simple. The greatest difficulty of the process under investigation is, in fact, that of having enough Brønsted acidity for the following steps. This is evident considering that the conversion of the starting substrate does not change when the experimental conditions are varied, while the selectivity in FAL increases considerably up to 69% when the temperature is decreased. The fact that at lower temperature there are no further products with respect to the ones in Figure 5 is noteworthy too (Σselectivities = 100%). This implies that the undesired products require higher temperature to be formed.
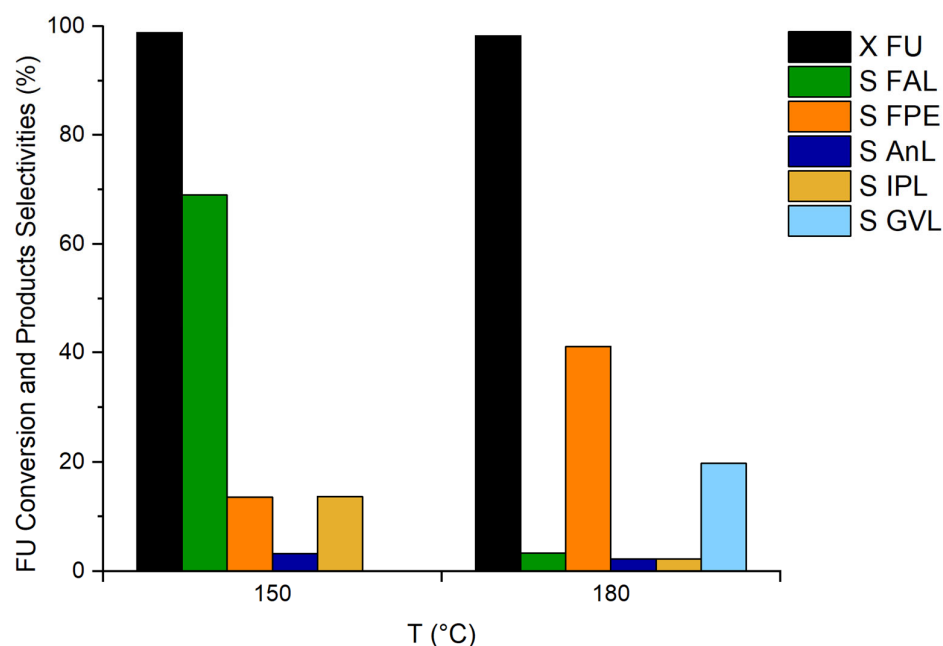
Figure 9. Furfural conversion and product selectivity trends as a function of reaction temperature (°C) using Ti/Zr/O (1:1). Reaction conditions: [FU] = 67 mM, τ = 10 min, m_{cat} = 0.76 g.

The influence of contact time was also evaluated by varying the flow rate (Figure 10) and keeping the temperature at 180 °C. Given that the conversion was complete with τ = 10 min, two tests at lower values were taken into consideration: 2.5 and 5 min. The study allowed the identification of a trend in product selectivity tendencies: as the contact time increases, the selectivity in FPE and GVL increases, while the one in FAL decreases. FU conversion is greater than 96% in all cases. Evidently, 2.5 min is not enough to form the desired products (S_{FAL} = 51%, S_{FPE} = 10%, S_{GVL} < 2%). The substrate needs more time to interact with the catalyst to be converted to successive intermediates. In fact, working with τ = 5 min, the selectivities in FPE and GVL increase to 31% and 11%, respectively. Unexpectedly, the sum of all values of selectivities is lower than the one at 10 min, indicating a higher amount of undesired products with respect to the test at a higher contact time. One more test with a contact time between 5 and 10 min could be useful to better understand this trend.

3.4. Study of the Reaction Mechanism

To better comprehend the reaction pathway that leads from FU to GVL under the conditions used, the reaction mechanism was evaluated using the principal intermediates identified in previous tests as substrates. Four tests were then carried out starting from FAL, furfuryl ethyl ether (FEE), propyl levulinate (PL) and AnL. It was not possible to use FPE and IPL, which are the real intermediates of the reaction under examination, as these products are not commercially available. Instead, the most similar commercial products were used, respectively FEE and PL. Catalytic tests were carried out for about 9 h in order to obtain stable results and verify the possible deactivation of the catalyst in the presence of a specific intermediate. Figure 11 shows the average results obtained.

Using FAL as a starting molecule, mainly FPE is produced with a selectivity of 41%. GVL is also obtained, reaching a selectivity value slightly under 20%. As expected, the results obtained for FAL are very similar to those exhibited by the test where FU was used as a starting substrate. In fact, given the high Lewis acidity of these oxides [37,51], the first step of reduction (Figure 5) takes place with simplicity, so that the aldehyde is almost completely converted into the corresponding alcohol, which is in turn transformed into the subsequent products. The test using FEE as a starting compound allowed the most impeded step in the cascade process to be identified. This substrate, in fact, does

not convert at all. The reason probably lies in the fact that conversion of the ester into the levulinate requires Brønsted acidity [47], which is not strong enough to catalyze this step [37,51]. Given the reaction pattern in Figure 5, this suggests that the GVL produced in previous tests does not come from FPE conversion, but from AnL or IPL conversion. In fact, these two intermediates are in equilibrium with each other (Figure 12), and both easily form GVL, as shown by the results obtained from the tests carried out using these molecules as a substrate (Figure 11), where selectivity in GVL is higher than 72% and little quantities of IPL are produced ($S_{IPL} \approx 7\%$). Hence, the final product can derive directly from AnL or from its conversion into IPL. In any case, this last step occurs more easily than the previous one as it needs the presence of Lewis acid sites [47].
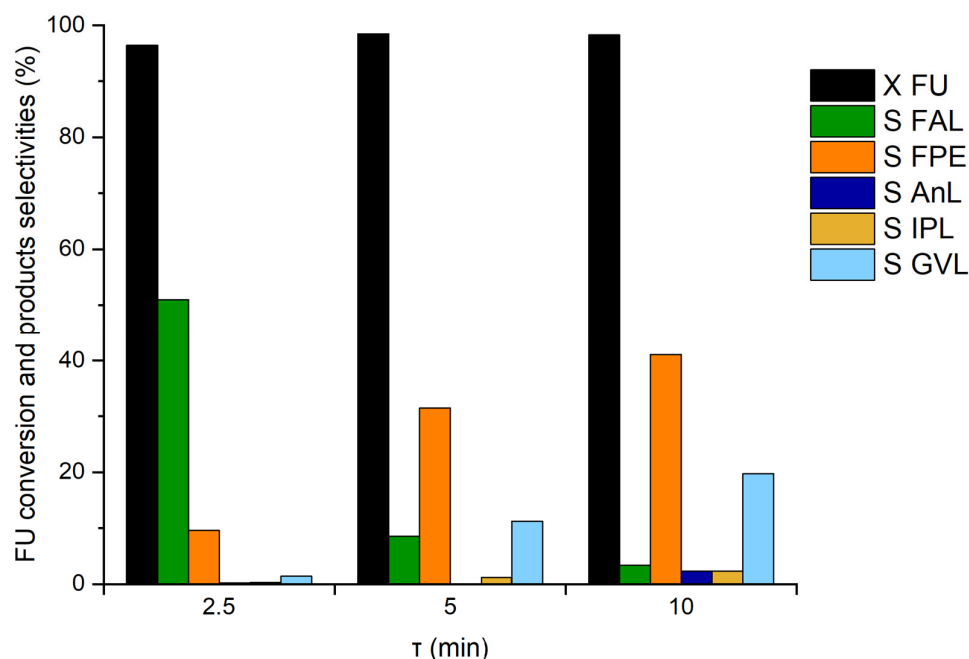

Figure 10. Furfural conversion and product selectivity trends as a function of contact time (min) using Ti/Zr/O (1:1). Reaction conditions: [FU] = 67 mM, T = 180 °C, m_{cat} = 0.76.
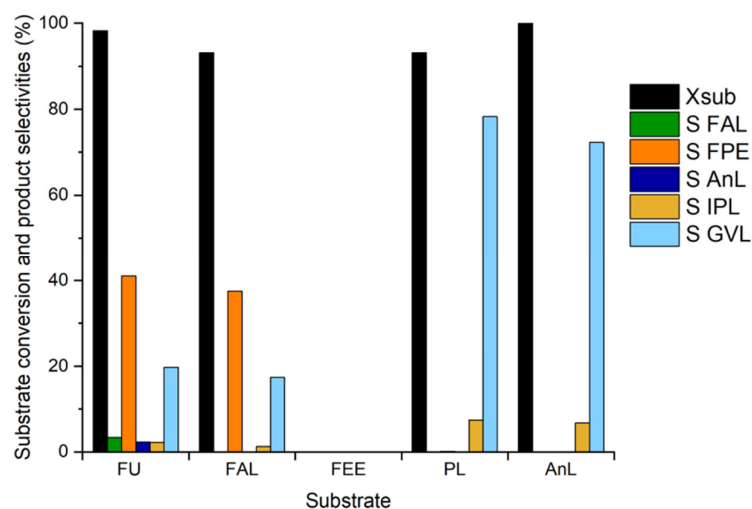

Figure 11. Comparison between substrate conversion and product selectivity trends obtained using the principal intermediates as substrates for the production of γ-valerolactone on Ti/Zr/O (1:1). Reaction conditions: [substrate] = 67 mM; τ = 10 min, T = 180 °C, m_{cat} = 0.76 g.
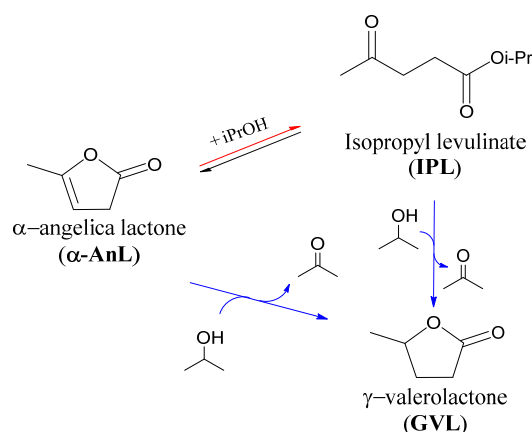
Figure 12. Simplified scheme of angelica lactone transformation in GVL and IPL. Blue arrows indicate the need for Lewis acidity while red arrows indicate the need for Brønsted acidity.

4. Conclusions

In the present work, Ti/Zr/O mixed oxides with different Ti/Zr molar ratios were prepared by co-precipitation at controlled pH. The results of characterization analysis using XRD, BET and NH_3-TPD methods were in good agreement with previous literature. Furthermore, an interesting trend was observed as the highest density of acid sites was associated with the lowest strength of acid sites. The catalytic performance of mixed oxides was investigated in the conversion of furfural to γ-valerolactone in a liquid-phase continuous reactor. Ti/Zr/O with 1:1 molar ratio was not only identified as the best material in terms of superficial area and acidity loading but also demonstrated to have the highest catalytic activity in terms of selectivity for the desired products and long-term catalytic performance. Furthermore, it was shown to be stable. In fact, this catalyst managed to successfully catalyze four consecutive steps of the cascade reaction, maintaining remarkably stable performances (S_{GVL} = 20%, S_{FPE} = 41%, X_{FU} = 98%) for the entire duration of the tests (up to 52 h, T = 180 °C, τ = 10 min). In addition, after studying the influence of reaction conditions on Ti/Zr/O (1:1) performance, a temperature of 180 °C and a time of contact of 10 min were found to be suitable for the reaction under examination. The analysis of the reaction mechanism was also useful to understand the actual GVL formation pathway. In conclusion, the use of the CTH mechanism as an alternative to gaseous H_2 with cheaper catalysts and above all the implementation of the one-pot reaction in a liquid-phase continuous plant could represent the first steps towards the development of a more ambiently and economically sustainable process. In the future, further analysis of the samples to quantify Lewis acidity and the desired B/L acid ratio will be carried out for elucidating structure–activity relationships in more detail.

Supplementary Materials: The following supporting information can be downloaded at: https://www.mdpi.com/article/10.3390/chemengineering7020023/s1, Table S1: List of compounds used and their quantities for the mother solution; Table S2: Concentrations of the standards prepared for each individual compound from its mother solution; Figure S1: XRD patterns of the synthesized zirconia calcined at different temperatures. In green, the reference pattern of tetragonal zirconia from PDF 50-1089; Figure S2: XRD patterns of catalyst before and after reaction Ti/Zr/O (1:1); Figure S3: (a) N_2 adsorption−desorption isotherms and (b) pore size distribution of Ti/Zr/O (1:1) before and after (SPENT) reaction; Figure S4: Furfural conversion and product selectivities (%) as a function of time (h) using SiC. Reaction conditions: [FU] = 67 mM, τ = 10 min, T = 180 °C, m_{cat} = 0.75 g; Figure S5: Furfural conversion and product selectivities (%) as a function of time (h) using ZrO_2. Reaction conditions: [FU] = 67 mM, τ = 10 min, T = 180 °C, m_{cat} = 0.86 g; Figure S6: Furfural conversion and product selectivities (%) as a function of time (h) using TiO_2. Reaction conditions: [FU] = 67 mM, τ = 10 min, T = 180 °C, m_{cat} = 0.97 g.

References

1. López-Asensio, R.; Cecilia, R.A.; Jiménez-Gómez, C.P.; García-Sancho, C.; Moreno-Tost, R.; Mairelles-Torres, P. Selective production of furfuryl alcohol from furfural by catalytic transfer hydrogenation over commercial aluminas. *Appl. Catal. A Gen.* **2018**, *556*, 1–9. [CrossRef]

2. Jaswal, A.; Singh, P.P.; Mondal, T. Furfural—A Versatile, Biomass-Derived Platform Chemical for the Production of Renewable Chemicals. *Green Chem.* **2022**, *24*, 510–551. [CrossRef]

3. Marçon, H.M.; Pastre, J.C. Continuous Flow Meerwein–Ponndorf–Verley Reduction of HMF and Furfural Using Basic Zirconium Carbonate. *RSC Adv.* **2022**, *12*, 7980–7989. [CrossRef]

4. Zhang, T.; Li, W.; Xiao, H.; Jin, Y.; Wu, S. Recent Progress in Direct Production of Furfural from Lignocellulosic Residues and Hemicellulose. *Bioresour. Technol.* **2022**, *354*, 127126. [CrossRef] [PubMed]

5. Zhou, Q.; Liu, Z.; Wu, T.Y.; Zhang, L. Furfural from Pyrolysis of Agroforestry Waste: Critical Factors for Utilisation of C5 and C6 Sugars. *Renew. Sustain. Energy Rev.* **2023**, *176*, 113194. [CrossRef]

6. Wang, Y.; Zhao, D.; Liang, R.; Triantafyllidis, K.S.; Yang, W.; Len, C. Transfer Hydrogenation of Furfural to Furfuryl Alcohol over Modified Zr-Based Catalysts Using Primary Alcohols as H-Donors. *Mol. Catal.* **2021**, *499*, 111199. [CrossRef]

7. Mariscal, R.; Maireles-Torres, P.; Ojeda, M.; Sádaba, I.; López Granados, M. Furfural: A Renewable and Versatile Platform Molecule for the Synthesis of Chemicals and Fuels. *Energy Environ. Sci.* **2016**, *9*, 1144–1189. [CrossRef]

8. Martin Alonso, D.; Wettstein, S.G.; Dumesic, J.A. Gamma-Valerolacton, A Sustainable Platform Molecule Derived from Lignocellulosic Biomass. *Green Chem.* **2013**, *15*, 584–595. [CrossRef]

9. Melero, J.A.; Morales, G.; Iglesias, J.; Paniagua, M.; López-Aguado, C.; Wilson, K.; Osatiashtiani, A. Efficient One-Pot Production of γ-Valerolactone from Xylose over Zr-Al-Beta Zeolite: Rational Optimization of Catalyst Synthesis and Reaction Conditions. *Green Chem.* **2017**, *19*, 5114–5121. [CrossRef]

10. García, A.; Miguel, P.J.; Ventimiglia, A.; Dimitratos, N.; Solsona, B. Optimization of the Zr-loading on siliceous support catalysts leads to a suitable Lewis/Brønsted acid sites ratio to produce high yields to γ-valerolactone from furfural in one-pot. *Fuel* **2022**, *324*, 124549. [CrossRef]

11. Tian, Y.; Zhang, F.; Wang, J.; Cao, L.; Han, Q. A Review on Solid Acid Catalysis for Sustainable Production of Levulinic Acid and Levulinate Esters from Biomass Derivatives. *Bioresour. Technol.* **2021**, *342*, 125977. [CrossRef] [PubMed]

12. He, J.; Li, H.; Lu, Y.-M.; Liu, Y.-X.; Wu, Z.-B.; Hu, D.-Y.; Yang, S. Cascade Catalytic Transfer Hydrogenation–Cyclization of Ethyl Levulinate to γ-Valerolactone with Al–Zr Mixed Oxides. *Appl. Catal. Gen.* **2016**, *510*, 11–19. [CrossRef]

13. Gilkey, M.J.; Xu, B. Heterogeneous Catalytic Transfer Hydrogenation as an Effective Pathway in Biomass Upgrading. *ACS Catal.* **2016**, *6*, 1420–1436. [CrossRef]

14. Espro, C.; Gumina, B.; Szumelda, T.; Paone, E.; Mauriello, F. Catalytic Transfer Hydrogenolysis as an Effective Tool for the Reductive Upgrading of Cellulose, Hemicellulose, Lignin, and Their Derived Molecules. *Catalysts* **2018**, *8*, 313. [CrossRef]

15. Zhang, Y.; Gyngazova, M.S.; Lolli, A.; Grazia, L.; Tabanelli, T.; Cavani, F.; Albonetti, S. Chapter 10—Hydrogen Transfer Reaction as an Alternative Reductive Process for the Valorization of Biomass-Derived Building Blocks. In *Studies in Surface Science and Catalysis*; Albonetti, S., Perathoner, S., Quadrelli, E.A., Eds.; Horizons in Sustainable Industrial Chemistry and Catalysis; Elsevier: Amsterdam, The Netherlands, 2019; Volume 178, pp. 195–214. [CrossRef]

16. Islam, M.J.; Granollers Mesa, M.; Osatiashtiani, A.; Taylor, M.J.; Manayil, J.C.; Parlett, C.M.A.; Isaacs, M.A.; Kyriakou, G. The Effect of Metal Precursor on Copper Phase Dispersion and Nanoparticle Formation for the Catalytic Transformations of Furfural. *Appl. Catal. B Environ.* **2020**, *273*, 119062. [CrossRef]

17. Assary, R.S.; Curtiss, L.A.; Dumesic, J.A. Exploring Meerwein–Ponndorf–Verley Reduction Chemistry for Biomass Catalysis Using a First-Principles Approach. *ACS Catal.* **2013**, *3*, 2694–2704. [CrossRef]

18. Reddy, B.M.; Khan, A. Recent Advances on TiO_2-ZrO_2 Mixed Oxides as Catalysts and Catalyst Supports. *Catal. Rev.* **2005**, *47*, 257–296. [CrossRef]

19. Peng, L.; Gao, X.; Yu, X.; Li, H.; Zhang, J.; He, L. Facile and High-Yield Synthesis of Alkyl Levulinate Directly from Furfural by Combining Zr-MCM-41 and Amberlyst-15 without External H_2. *Energy Fuels* **2018**, *33*, 330–339. Available online: https://pubs.acs.org/doi/10.1021/acs.energyfuels.8b03422 (accessed on 22 January 2023). [CrossRef]

20. Zhang, J.; Liu, Y.; Yang, S.; Wei, J.; He, L.; Peng, L.; Tang, X.; Ni, Y. Highly Selective Conversion of Furfural to Furfural Alcohol or Levulinate Ester in One Pot over ZrO_2@SBA-15 and Its Kinetic Behavior. ACS Sustain. *Chem. Eng.* **2020**, *8*, 5584–5594. [CrossRef]

21. Cheng, Y.; Liu, Y.; Zhang, J.; Huang, R.; Wang, Y.; Cao, S.; He, L.; Peng, L. Acetic Acid-Regulated Mesoporous Zirconium-Furandicarboxylate Hybrid with High Lewis Acidity and Lewis Basicity for Efficient Conversion of Furfural to Furfuryl Alcohol. *Renew. Energy* **2022**, *184*, 115–123. [CrossRef]

22. Xie, W.; Gao, C.; Li, J. Sustainable Biodiesel Production from Low-Quantity Oils Utilizing $H_6PV_3MoW_8O_{40}$ Supported on Magnetic Fe_3O_4/ZIF-8 Composites. *Renew. Energy* **2021**, *168*, 927–937. [CrossRef]

23. Ronda-Leal, M.; Osman, S.M.; Won Jang, H.; Shokouhimehr, M.; Romero, A.A.; Luque, R. Selective Hydrogenation of Furfural Using TiO_2-Fe_2O_3/C from Ti-Fe-MOFs as Sacrificial Template: Microwave vs. Continuous Flow Experiments. *Fuel* **2023**, *333*, 126221. [CrossRef]

24. Lolli, A.; Zhang, Y.; Basile, F.; Cavani, F.; Albonetti, S. Beyond H2: Exploiting H-Transfer Reaction as a Tool for the Catalytic Reduction of Biomass. In *Chemicals and Fuels from Bio-Based Building Blocks*; John Wiley & Sons, Ltd.: Hoboken, NJ, USA, 2016; pp. 349–378. [CrossRef]

25. Vásquez, P.B.; Tabanelli, T.; Monti, E.; Albonetti, S.; Bonincontro, D.; Dimitratos, N.; Cavani, F. Gas-Phase Catalytic Transfer Hydrogenation of Methyl Levulinate with Ethanol over ZrO_2. *ACS Sustain. Chem. Eng.* **2019**, *7*, 8317–8330. [CrossRef]

26. Winoto, H.P.; Ahn, B.S.; Jae, J. Production of γ-Valerolactone from Furfural by a Single-Step Process Using Sn-Al-Beta Zeolites: Optimizing the Catalyst Acid Properties and Process Conditions. *J. Ind. Eng. Chem.* **2016**, *40*, 62–71. [CrossRef]

27. Hernández, B.; Iglesias, J.; Morales, G.; Paniagua, M.; López-Aguado, C.; García Fierro, J.L.; Wolf, P.; Hermans, I.; Melero, J.A. One-Pot Cascade Transformation of Xylose into γ-Valerolactone (GVL) over Bifunctional Brønsted–Lewis Zr–Al-Beta Zeolite. *Green Chem.* **2016**, *18*, 5777–5781. [CrossRef]

28. López-Aguado, C.; Paniagua, M.; Melero, J.A.; Iglesias, J.; Juárez, P.; López Granados, M.; Morales, G. Stable Continuous Production of γ-Valerolactone from Biomass-Derived Levulinic Acid over Zr–Al-Beta Zeolite Catalyst. *Catalysts* **2020**, *10*, 678. [CrossRef]

29. Melero, J.A.; Morales, G.; Iglesias, J.; Paniagua, M.; López-Aguado, C. Rational Optimization of Reaction Conditions for the One-Pot Transformation of Furfural to γ-Valerolactone over Zr–Al-Beta Zeolite: Toward the Efficient Utilization of Biomass. *Ind. Eng. Chem. Res.* **2018**, *57*, 11592–11599. [CrossRef]

30. Al Azri, N.; Patel, R.; Ozbuyukkaya, G.; Kowall, C.; Cormack, G.; Proust, N.; Enick, R.; Veser, G. Batch-to-Continuous Transition in the Specialty Chemicals Industry: Impact of Operational Differences on the Production of Dispersants. *Chem. Eng. J.* **2022**, *445*, 136775. [CrossRef]

31. Bukhtiyarova, M.V.; Bukhtiyarova, G.A. Reductive Amination of Levulinic Acid or Its Derivatives to Pyrrolidones over Heterogeneous Catalysts in the Batch and Continuous Flow Reactors: A Review. *Renew. Sustain. Energy Rev.* **2021**, *143*, 110876. [CrossRef]

32. Tabanelli, T.; Paone, E.; Blair Vásquez, P.; Pietropaolo, R.; Cavani, F.; Mauriello, F. Transfer Hydrogenation of Methyl and Ethyl Levulinate Promoted by a ZrO_2 Catalyst: Comparison of Batch vs Continuous Gas-Flow Conditions. *ACS Sustain. Chem. Eng.* **2019**, *7*, 9937–9947. [CrossRef]

33. Komanoya, T.; Nakajima, K.; Kitano, M.; Hara, M. Synergistic Catalysis by Lewis Acid and Base Sites on ZrO_2 for Meerwein–Ponndorf–Verley Reduction. *J. Phys. Chem. C* **2015**, *119*, 26540–26546. [CrossRef]

34. Schiller, R.; Weiss, C.K.; Landfester, K. Phase Stability and Photocatalytic Activity of Zr-Doped Anatase Synthesized in Miniemulsion. *Nanotechnology* **2010**, *21*, 405603. [CrossRef] [PubMed]

35. Zhao, D.; Su, T.; Rodríguez-Padrón, D.; Lü, H.; Len, C.; Luque, R.; Yang, Z. Efficient Transfer Hydrogenation of Alkyl Levulinates to γ-Valerolactone Catalyzed by Simple Zr–TiO_2 Metal Oxide Systems. *Mater. Today Chem.* **2022**, *24*, 100745. [CrossRef]

36. De, S.; Dutta, S.; Saha, B. Critical Design of Heterogeneous Catalysts for Biomass Valorization: Current Thrust and Emerging Prospects. *Catal. Sci. Technol.* **2016**, *6*, 7364–7385. [CrossRef]

37. Wan, J.; Fu, L.; Yang, H.; Wang, K.; Xi, F.; Pan, L.; Li, Y.; Liu, Y. TiO_2–ZrO_2 Composite Oxide as an Acid–Base Bifunctional Catalyst for Self-Condensation of Cyclopentanone. *Ind. Eng. Chem. Res.* **2020**, *59*, 19918–19928. [CrossRef]

38. Rao, K.N.; Reddy, B.M.; Park, S.-E. Novel CeO_2 Promoted TiO_2–ZrO_2 Nano-Oxide Catalysts for Oxidative Dehydrogenation of p-Diethylbenzene Utilizing CO_2 as Soft Oxidant. *Appl. Catal. B Environ.* **2010**, *100*, 472–480. [CrossRef]

39. Lin, F.; Jiang, X.; Boreriboon, N.; Song, C.; Wang, Z.; Cen, K. CO_2 Hydrogenation to Methanol over Bimetallic Pd-Cu Catalysts Supported on TiO_2-CeO_2 and TiO_2-ZrO_2. *Catal. Today* **2021**, *371*, 150–161. [CrossRef]

40. Reddy, B.M.; Lee, S.-C.; Han, D.-S.; Park, S.-E. Utilization of Carbon Dioxide as Soft Oxidant for Oxydehydrogenation of Ethylbenzene to Styrene over V_2O_5–CeO_2/TiO_2–ZrO_2 Catalyst. *Appl. Catal. B Environ.* **2009**, *87*, 230–238. [CrossRef]

41. Raj, K.J.A.; Viswanathan, B. Effect of Surface Area, Pore Volume and Particle Size of P25 Titania on the Phase Transformation of Anatase to Rutile. *Indian J. Chem.* **2009**, *48*, 1378–1382.

42. Watanabe, S.; Ma, X.; Song, C. Characterization of Structural and Surface Properties of Nanocrystalline TiO_2−CeO_2 Mixed Oxides by XRD, XPS, TPR, and TPD. *J. Phys. Chem. C* **2009**, *113*, 14249–14257. Available online: https://pubs.acs.org/doi/10.1021/jp8110309# (accessed on 24 January 2023). [CrossRef]

43. Lu, M.; Du, H.; Wei, B.; Zhu, J.; Li, M.; Shan, Y.; Shen, J.; Song, C. Hydrodeoxygenation of Guaiacol on Ru Catalysts: Influence of TiO_2–ZrO_2 Composite Oxide Supports. *Ind. Eng. Chem. Res.* **2017**, *56*, 12070–12079. [CrossRef]

44. Khanna, P.K.; Singh, N.; Charan, S. Synthesis of Nano-Particles of Anatase-TiO_2 and Preparation of Its Optically Transparent Film in PVA. *Mater. Lett.* **2007**, *61*, 4725–4730. [CrossRef]

45. Tajima, M.; Niwa, M.; Fujii, Y.; Koinuma, Y.; Aizawa, R.; Kushiyama, S.; Kobayashi, S.; Mizuno, K.; Ohuchi, H. Decomposition of Chlorofluorocarbons on TiO_2ZrO_2. *Appl. Catal. B Environ.* **1997**, *12*, 263–276. [CrossRef]

46. Manríquez, M.E.; López, T.; Gómez, R.; Navarrete, J. Preparation of TiO_2–ZrO_2 Mixed Oxides with Controlled Acid–Basic Properties. *J. Mol. Catal. Chem.* **2004**, *220*, 229–237. [CrossRef]

47. Zhang, H.; Yang, W.; Roslan, I.I.; Jaenicke, S.; Chuah, G.-K. A Combo Zr-HY and Al-HY Zeolite Catalysts for the One-Pot Cascade Transformation of Biomass-Derived Furfural to γ-Valerolactone. *J. Catal.* **2019**, *375*, 56–67. [CrossRef]

48. Iglesias, J.; Melero, J.A.; Morales, G.; Paniagua, M.; Hernández, B.; Osatiashtiani, A.; Lee, A.F.; Wilson, K. ZrO_2-SBA-15 Catalysts for the One-Pot Cascade Synthesis of GVL from Furfural. *Catal. Sci. Technol.* **2018**, *8*, 4485–4493. [CrossRef]

49. García, A.; Miguel, P.J.; Pico, M.P.; Álvarez-Serrano, I.; López, M.L.; García, T.; Solsona, B. γ-Valerolactone from Levulinic Acid and Its Esters: Substrate and Reaction Media Determine the Optimal Catalyst. *Appl. Catal. Gen.* **2021**, *623*, 118276. [CrossRef]

50. Kikhtyanin, O.; Kelbichová, V.; Vitvarová, D.; Kubů, M.; Kubička, D. Aldol Condensation of Furfural and Acetone on Zeolites. *Catal. Today* **2014**, *227*, 154–162. [CrossRef]

51. García-Olmo, A.; Yepez, A.; Balu, A.; Romero, A.; Luque, R. Insights into the Activity, Selectivity and Stability of Heterogeneous Catalysts in the Continuous Flow Hydroconversion of Furfural to Valuable Products. *Catal. Sci. Technol.* **2016**, *6*, 4705–4711. [CrossRef]